Multiple User Recognition with Passive RFID Tomography

Benjamin Wagner, Tobias Ritt and Dirk Timmermann

***Abstract*— The positioning and tracing of multiple users is an important data source for ubiquitous assistance in smart environments and its superimposed intention recognition systems. Within application areas like elderly care or ambient assisted living, non-invasive, wireless, privacy preserving technologies are indispensable. Device-free localization approaches (DFL) provide these advantages with no need for user-attached hardware.**

In our recent work we provide a passive RFID enabled and radio tomography based approach, which combines privacy and cost effectiveness. Within our previous proof of concepts only one user scenarios were investigated. An open problem within the DFL research is the recognition and distinction of multiple users.

In this work we show related approaches and define methods and algorithms for multi user support. We conduct experiments in an indoor room DFL scenario for proof of concept and validation. We show that it is possible to recognize and distinct up to 3 users with reasonable precision.

***Index Terms*— DFL, RFID, Indoor Navigation, Smart Environments, Pervasive Computing, Wireless**

I. INTRODUCTION

IN indoor smart environments it is important to know the number and position of different users to provide assistance. Creating inexpensive, wireless, privacy preserving systems is the aim of device-free user localization (DFL). Compared to the much broader research in sensor localization, very little research has been presented in locating users who do not have to wear any devices. Within the DFL research most proposed systems use an active radio infrastructure within the room influenced by the user´s body. In our recent work we combine several method and technologies to a new encouraging approach named Passive RFID Tomography[1]. Based on the *Radio Tomographic Imaging* technique (RTI) introduced by Wilson and Patwari [2], [3] this technology applies an imaging approach to an industrial Passive Radio Frequency Identification System (pRFID). While a person is moving within the measurement area the radio links are influenced and the path loss gives information about the location and the movement of the user. The architecture consists of completely *passive Radio Frequency Identification* transponders (pRFID) and only a few active RFID reader antennas leading to three main advantages:

1. Low Cost: transponders can be purchased for ~ 0.2 €
2. Low maintenance: no batteries needed, easy placement i.e. under the carpet or wallpaper
3. Adaptive precision: higher resolution through higher transponder density

However recent experimental work only regards one user scenarios, although in reality almost more users are interacting with each other in the environment.

The new approach presented in this work proposes methods for recognizing, localizing and tracing multiple users within the measurement area.

This paper is structured as follows: in Section II the related techniques and the state of the art of pRFID and multi target RTI are described. Section III gives information about the methods and algorithms we used, followed by the experimental validation in Section IV. We show our results in V and conclude with Section VI.

II. RELATED WORK

The work presented in this publication is mainly based on two different recent works: the passive RFID Tomography by Wagner, Patwari et al.[1] and the Multi User Approaches of Bocca et al.[4].

A. *Passive RFID Tomography*

Using typical RFID hardware provides less signal processing possibilities than typically used wireless sensor nodes. For this reason our measurements regards the *Received Signal Strength Indicator* (RSSI) which can be regarded as a linear transformation of the original signal strength value.

As shown by Lieckfeldt et al. [5] the presence of the human body does strongly affect the communication between the RFID reader hardware and the passive transponders. This can be modeled as[5]:

$$\Delta P(d_{exc}) = A d_{exc}^{B} \cos\left(\frac{2\pi}{\lambda} d_{exc} + \phi_{refl}\right) \qquad (1)$$

with ΔP as estimated RSSI change, wave length λ and phase shift ϕ_{refl}. The parameters A,B are subject to the multipath

This work was partially financed by the German Research Foundation (DFG) within the graduate school Multimodal Smart Appliance ensembles for Mobile Applications (MuSAMA, GRK 1424).

B. Wagner is with the Institute of Applied Microelectronics and Computer Engineering at the University of Rostock, Germany (phone: 049-381-498-7271; fax: 049-381-498-1187251; e-mail: benjamin.wagner@uni-rostock.de).

D. Timmermann is head of the Institute of Applied Microelectronics and Computer Engineering at the University of Rostock, Germany. (e-mail: dirk.timmermann@uni-rostock.de).

T. Ritt received his B.Sc. at the Institute of Applied Microelectronics and Computer Engineering at the University of Rostock, Germany in 2014. (e-mail: tobias.ritt@uni-rostock.de).

fading properties of the experimental environment[6]. Therefore the model needs to be re-adjusted for every new setup.

The path difference d_{exc} between the Line-of-sight (LOS) and the Non-Line-of-sight (NLOS) path is determining the relative position of a scattering user towards a specific communication link.

In our recent work [1] wireless sensor network based radio tomographic imaging [2], [3] and RFID DFL were combined. The setup consists of waist-high mounted passive transponders placed around the discretized measurement area. The RFID antennas are placed directly behind the transponder lines to guarantee a maximum power transfer.

The imaging result is calculated by using the model of Wilson et.al.[2]:

$$\Delta y = W\Delta x + n \tag{2}$$

with Δy as matrix of RSS differences in dB, W as pre-calculated weighting matrix for every pixel-link-combination, n as zero mean gaussian noise vector and Δx as matrix of pixel attenuations generating a tomographic picture of the measurement area.

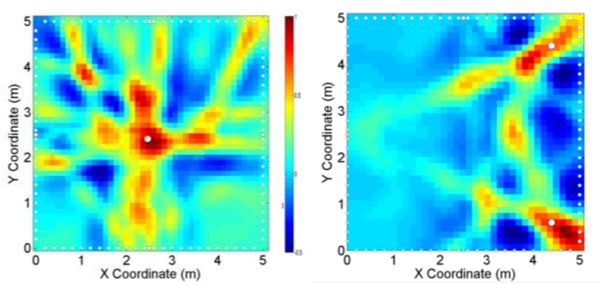

(1) (2)

Figure 1. RFID Image for (1) 1 User (2) 2 Users

The algorithm can locate humans with as low as 0.3 m mean location error. In [8] we propose multiple improvements for performance and online operation. Fig.1 is showing a standard pRFID tomography image for a 1 and a 2 user scenario. It can be easily seen, that in (1) the user can be easily estimated by just using the maximum pixel, that isn´t possible in (2) because of multiple maxima.

B. *Multiple Target Tracking in WSNs*

Like the original RTI Approach of [2] Bocca, Kaltiokallio et al. are using Wireless Sensor Nodes (WSN) for the evaluation. This has several differences from working with RFID. The major advantages are: a high amount of sender-receiver pairings, an individual time slot optimized communication protocol and multi-channel capabilities. Based on these advantages a less noisy RTI image estimate can be used as the input for multiple target algorithms.

The explained method from [4] can be mainly divided into main parts:

1) *Denoising*

This is mainly the first step to be done to remove random small peak areas from the image, which are resulting out of the measurement procedure and obstruction capabilities of the room. Therefore it is common to use a gaussian filter with the standard deviation σ_d as resulting image Δx quality indicator.

2) *Tresholding*

In this step the number of input pixels for the clustering algorithm is reduced to only those pixels which are in the vicinity of a user in the field. Therefor a threshold value T_f is derived dynamically based on the average pixel attenuation from a former calibration phase:

$$T_f(t) = \begin{cases} \beta I_f(t) & if \quad |T(t)| > 0 \\ 2\overline{I_e} & otherwise \end{cases} \tag{3}$$

with the average calibration value $\overline{I_e}$, a low-pass filter threshold value $I_f(t)$ and a scaling factor β. Case 2 is used, if no former user presence estimation available ($|T(t)| = 0$), in every later step case 1 is derived. This is done in a recursive loop.

3) *Clustering*

The clustering step is assigning specific pixel sets to the associated *blobs* (joint pixel area forming a user's image attenuation). For this the hierarchical agglomerative clustering approach (HAC) from Hastie et al.[9] is used. It is an iterative merging algorithm starting with all pixels considered as independent up to building larger pixel clusters. The basic measure for the algorithm and the cluster size is the individual average Euclidean distance between the pixels. A threshold value T_C is predefined determining the average cluster diameter and its number.

In the last step the so called *cluster heads*, the pixel with the highest attenuation for every generated cluster are determined.

4) *Gating*

The gating procedure is done for managing changing user populations and tracking. Therefor certain *Gating Areas* are defined in the vicinity of the calculated pixel clusters on basis of a predefined dynamic radius r_t. After calculating a difference matrix between the former and the current estimation vector, the positions outside the gating area are set to ∞:

$$[\Omega]_k = \begin{cases} \|P_k - P_{k-1}\| & if \;\; P_k \in x_g \\ \infty & otherwise \end{cases} \tag{4}$$

with gating vector x_g and user positions P. In the last step the cost matrix $[\Omega]_k$ is optimized via Hungarian or Gready algorithm. If no new position estimation possible a Kalman filtering is used.

III. Methods

In this chapter we explain the method we used for estimating the number and the position of multiple users in our pRFID scenario and combine this estimate with a tracking procedure. The raw estimation approach is divided into a method with using a priori available knowledge about the number of present users and without.

A. *Multi-Channel RFID*

Even within industrial RFID technology it is possible to communicate on different channels. This is mainly defined for Multi-Reader-Environments. There the EPCglobal Gen2 Standard[10] defines 4 different Tx channels with neighbored Rx bands between 865 and 868 MHz for european use. Every channel has a bandwidth of 200 KHz. Fig. 2 is showing the standardized channel band allocation.

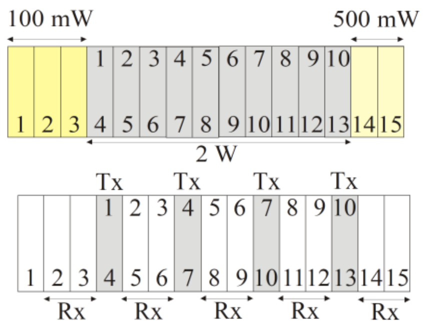

Figure 2. Channel allocation [7]

Evaluation RFID communication on these channels reveals no significant information contribution within the RSSI measurement. Fig. 3 is showing a simple experiment with a user going moving on one path between reader antenna and transponder in two opposite directions. A significant drop of field strength is apparent due to our mentioned physical model (cp. II.A), but no significant change due to the different channels.
A significant information contribution is possibly available in the signal phase information. This should be evaluated in further investigations since until now it was not possible to measure phase information with commercial RFID hardware.

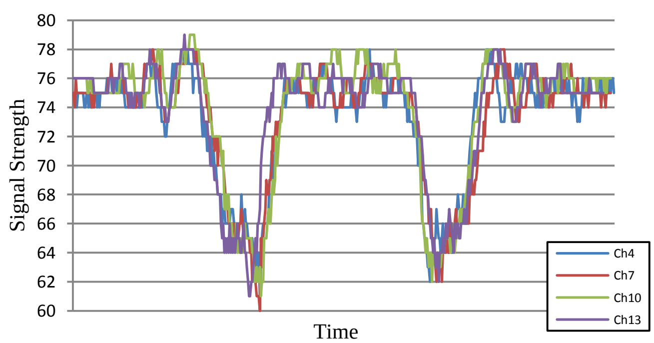

Figure 3. RSSI drop with a moving user on one path with 2 different orientations (forward / backward)

B. *Static Estimation without A Priori Knowledge*

Our starting point is the original pRFID image matrix. We implement a dynamic tresholding method, because the RFID technology has much more noise instabilities than multi-channel enabled WSN approaches (cp. Fig. 6). The threshold S_n is defined by:

$$S_n = \delta \max(\Delta x) \tag{5}$$

with the absolute image matrix maximum and a scaling factor δ, which is experimental determined.

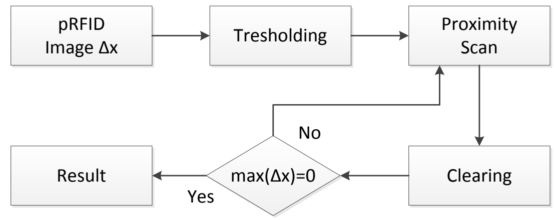

Figure 4. Flow diagram of static estimation without a priori knowledge about user number

In the next step the area in the proximity of the maximum pixel attenuation (radius r_U) is scanned to decide whether this attenuation area can be matched to a user or not (cp. Fig. 7). After getting the maximum pixel:

$$[x_{MAX}; \mathrm{y_{MAX}}] = \max(\Delta x) \tag{6}$$

the cluster around this is evaluated by the attenuation of each pixel. A counter $\aleph_P$ is incremented for every non-zero pixel attenuation and decremented for every positive value:

$$\aleph_P = \begin{cases} \aleph + 1 \; if \; \Delta x(i,j) > 0 \\ \aleph - 1 \; if \; \Delta x(i,j) = 0 \end{cases} \tag{7}$$

with i,j realizing the radius r_U around the maximum pixel. This is sketched in Fig. 4. Afterwards a threshold S_u is applied on $\aleph_P$ for user estimation, a higher counter value is implying a user's presence. In the next step the pixel cluster has to be cleared. If a person was recognized the whole cluster and additive pixels due to radius r_D are erased. This is done because real users are typically leading to higher attenuations in the field.
This procedure is done in a loop until no attenuation higher than zero is remaining in the filtered image.

C. *Static Estimation with A Priori Knowledge*

The basic algorithm is identical to the method without a priori information described above. In some environments it is possible to get the information about the number of present users out of the infrastructure, i.e. light barriers or other sensors at the door. This is now implemented as external input parameter.
Fig. 5 is showing the extended algorithm. A second reference image vector is built were only the estimated user clusters are cleared. Cluster which do not meet the requirements of user constitution are kept within the reference.

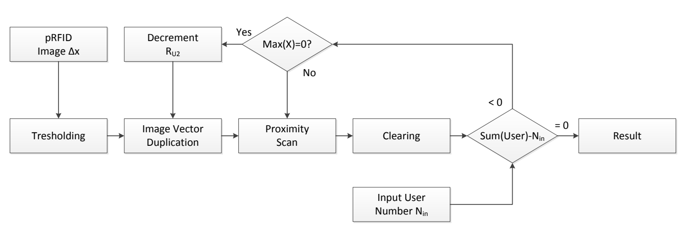

Figure 5. Flow chart of Static Estimation with a priori knowledge

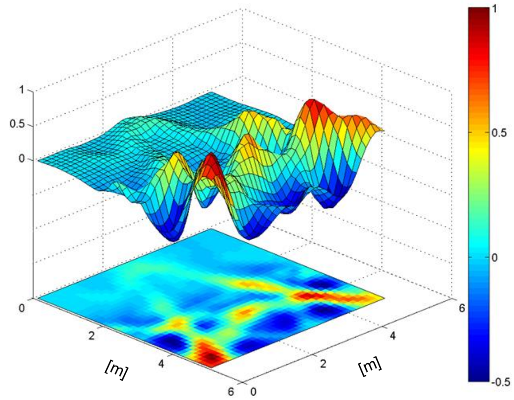

(1)

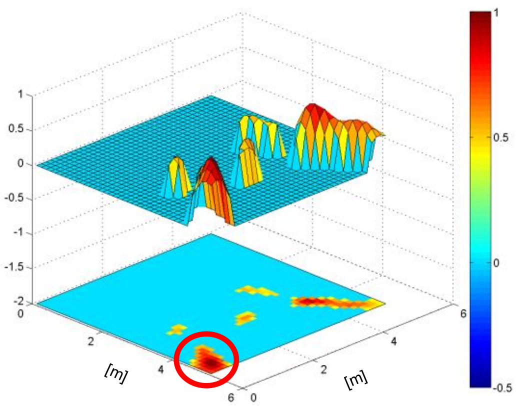

(2)

Figure 6. Original pRFID image with 2 users (1) and image after Tresholding (2)

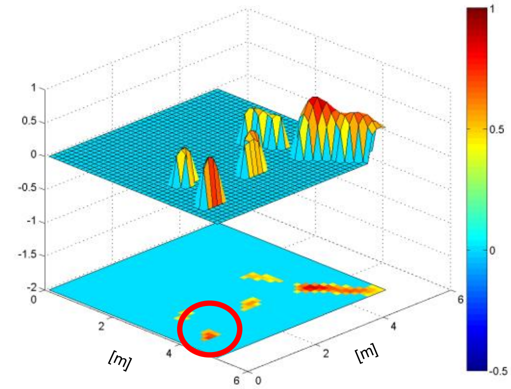

(1)

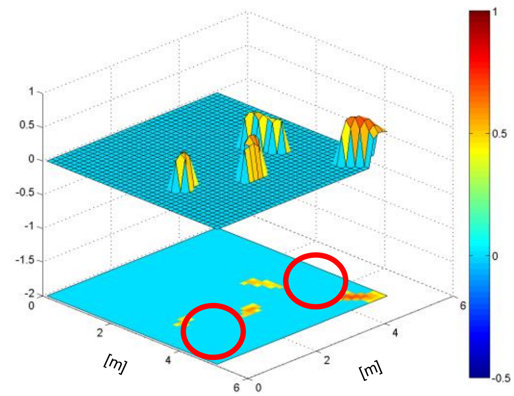

(2)

Figure 7. Filtered image after (1) Proximity Scan and (2) Clearing and next estimation round

After the recognition step there is checked whether all users given by the external user number sensor are recognized. If there are more users to be localized the algorithm is working until the image vector has no further positive attenuations.
Is the image vector completely cleared but there is a positive difference between recognized and a priori user number the radius R_{U2} is decremented about 1 pixel length D_{Pixel}. This is done until R_{U2} = D_{Pixel} and every user position is found.

D. *Dynamic Estimation*

The dynamic user estimation approach is applied on continuous pRFID tomography data. Our proposed algorithm distinguishes between 2 cases: (1) it is possible to estimate the next step position from the field data. (2) There is too much noise in the measurement (e.g. a user is blocking one RFID antenna) and the next position cannot be estimated out of the image data. In that case a Kalman Filter is activated to estimate the trajectory until the next imaging estimate is available.
The user number and position estimation is done with the algorithm described in III.B. The initial estimation vector is defining the overall number of users to be tracked. Therefor it is likely to define certain entry areas in the field (e.g. the field edges or the door area), where users first appear. The next steps are done for every distinct user trajectory. There is an implemented plausibility check, whether two users are standing on the same position. In that case there are intersecting trajectories and the next position is calculated by

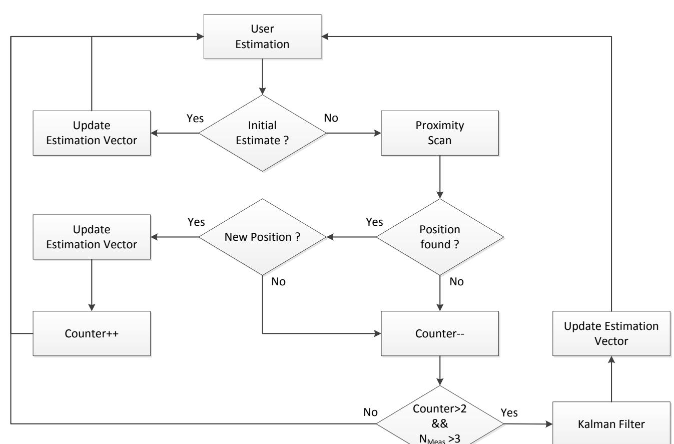

Figure 8. Schematic diagram of dynamic user estimation

the Kalman Filter. This is also done if no further image estimation is possible due to heavy noise. The counter parameter prevent from unnecessary tracing if a person is recognized wrong. In the current implementation the algorithm waits 2 counts out of 3 measurements before clearing a trace. The schematic is shown in Fig. 8.

IV. Experimental Validation

The major parts of the experimental setup are: a passive UHF RFID reader connected to a processing workstation via ethernet and a square field equipped with 96 passive paper transponders. We use a monostatic UHF reader from Kathrein Sachsen[11] working in the ISM 868 MHz frequency band and implementing the EPCglobal [10] Class-1 Generation-2 UHF RFID Protocol. The transponders are ALN-9640 Squiggle® Inlays from Alien Technology[12], specialized for general purpose use with high read ranges up to 10m. For transponder powering and the backward link communication four circular polarized UHF antennas with a gain of 8.5 dBic and a 69 degree azimuth beam width (WiRa70°) are used. For our measurements we installed a square field with hip height mounted UHF transponders with a 96-bit EPC[10] compliant memory holding a unique identification number. The RFID reader antennas are placed in the middle of every field side. Due to the beam width size and beam form of the chosen antenna we could realize a field size of 25 m², which is similar to a standard laboratory room (cp. Fig. 9). Every antenna is mainly powering the transponders of the opposite side. Due to that issue we can place the antenna in line with the separate field sides that makes an installation on room walls possible.

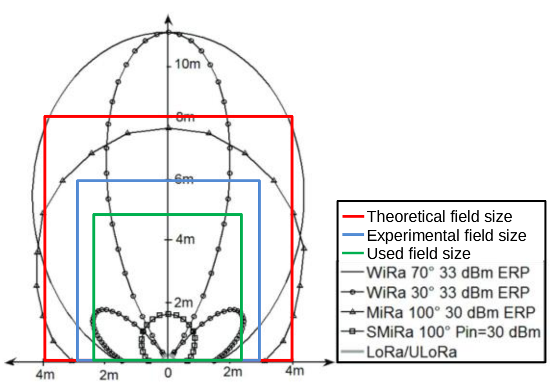

Figure 9. Field size and antenna beamsize comparison

The reader is communicating via ethernet with the operating workstation running a customized C program fetching the transponder data by a predefined inventory protocol. The processing station is a Unix running PC with an AMD®Phenom™2 X4 Quad CPU @ 4*3.4 GHz.

We placed 24 transponders at every field side resulting in a sum of 96 transponders on a height of 0.85 m. On the field we defined 13 testing user locations illustrated in Fig. 10. For getting enough data from every transponder we had to measure at least 20s per side. That time belongs to the ineffective industrial anti-collision protocol. So we were only able to measure a certain set of representative positions combinations.

Due to its monostatic radio architecture every antenna is powering the transponder line at the opposite side of the field and receiving the transponder answers on the neighbor narrow bands. This ensures a maximum and well balanced power transmission to the transponders.

The EPCglobal[10] UHF RFID communication protocol at 860-960 MHz defines baseband operations to address a smaller subset of RFID transponders. Using this functionality we implemented, a bitwise masking procedure available in the readers API. We divide the transponder population into 4 hexadecimal subgroups, one per field side.

$$Q = log_2(N) - 1 \tag{8}$$

In every inventory cycle 24 transponders are to be read, but all 96 transponders are reacting on the first inventory command before the masking starts. Therefor we choose a Q=6 as an optimal value, guaranteeing a maximum possible reading speed. We emphasized the length of each inventory round, to get a minimum of 10 data samples per transponder- antenna combination. For the calibration phase we implemented a minimum of 20 data samples to get a reliable mean signal strength value.

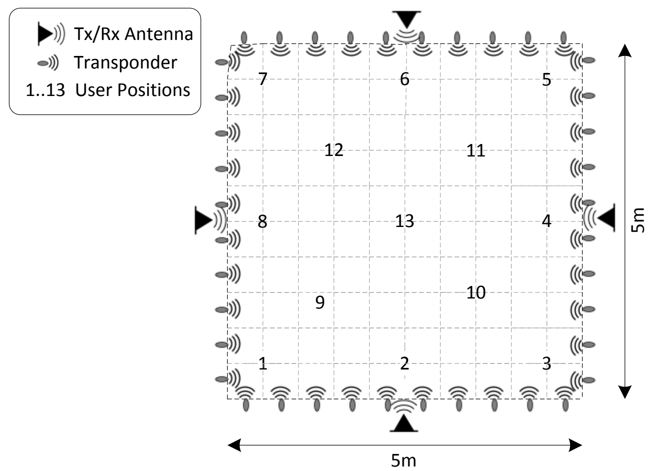

Figure 10. Experimental system structure (sketch)

The analysis is done by a MATLAB® program running on the workstation in a post processing step. The algorithmic parameters for the methods described in III are listed in Table I and were evaluated experimentally.

TABLE I
Algorithm Parameters

$\delta_{Estimation}$	0.4
$\delta_{Tracking}$	0.35
R_U	0.4 m
R_{U2}	0.53 m
R_D	1.2 m
S_U	-7
$R_{Tracking}$	0.68m
D_{Pixel}	0.13 m

V. Results

In Fig. 11 the CDFs of the proposed multi user approaches are shown. We only evaluated different combinations of 2 and 3 users. If there are 4 and more users present in the room, the accuracy drops dramatically. In that case only the field edges provide enough accuracy for localization. In Table II the particular accuracy values are shown. They should be regarded in the context of the original pRFID approach in [1] were we achieve an average error of 0.30 m within a 3x3m field and 1 present user. With 2 users the average error is 0.45m and 0.66m with 80% confidence is achieved within 5x5m. The accuracy is directly connected to the position within the field. Is the user is standing direct in the front of one antenna the accuracy drops down. In the worst case several antennas are blocked simultaneously with very noisy image results.

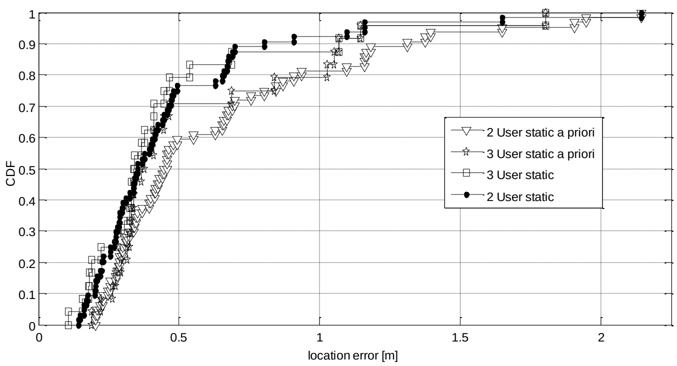

Figure 11. CDF of location error in 2 and 3 user scenarios

It is remarkable that the method with use of a priori knowledge about the user number the location error rises. This effect rises if more clusters are generated than users determined a priori. In that case the probability of false detection is very high and leads to higher inaccuracies.

TABLE II
ALGORITHM PARAMETERS

2 Users	Static	Static with a priori
Average Error	0.45 m	0.66 m
80% Confidence	0.66 m	1.00 m
User Number Error	0.41	0.00
3 Users		
Average Error	0.45 m	0.55 m
80% Confidence	0.55 m	1.00 m
User Number Error	0.46	0.04

The result of a sample user tracking scenario is shown in Fig. 12. Therefor 2 users are beginning to walk in opposite field edges and are moving with the same speed (~1 step per frame) towards each other. In the middle of the field the trajectories are crossing and they are moving further to the opposite edge. In the figure the result of the estimation process is also shown. It is noticeable that the algorithm provides reasonable tracking performance. If there is too much noise within the imaging data the trajectory is mainly determined by the Kalman Filter. In that case the method has weak results after the crossing trajectories.

VI. CONCLUSION

In this work we provide three different approaches for multiuser support in an innovative passive RFID based device-free localization system. Compared to the original approach the system can provide reasonable results around 0.45m for maximum 3 users for a 25m² indoor scenario. If there are more users to be tracked the number of active elements (reader antennas) should be increased in order to have a higher communication link density.

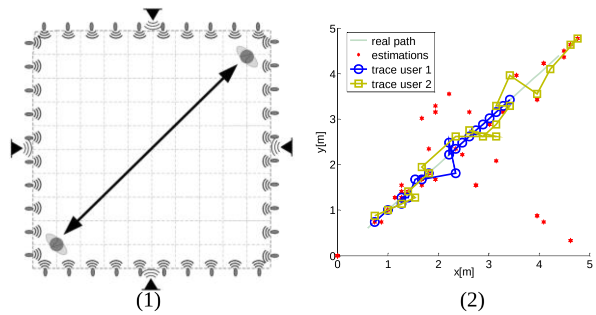

Figure 12. 2 User tracking scenario (1) and dynamic estimation result (2)

In further work we will investigate the use of phase information within the RFID base band signal for generating a higher amount of measurement information and try to increase the RFID transponder density by placing them on walls and furniture.

ACKNOWLEDGEMENT

We would like to thank Tobias Pohl and Sascha Rohde for their supporting experimental work.

REFERENCES

[1] B. Wagner, N. Patwari, and D. Timmermann, “Passive RFID tomographic imaging for device-free user localization,” *2012 9th Work. Positioning, Navig. Commun.*, 2012.

[2] J. Wilson and N. Patwari, “Radio Tomographic Imaging with Wireless Networks,” *IEEE Trans. Mob. Comput.*, May 2010.

[3] J. Wilson and N. Patwari, “Through-Wall Motion Tracking Using Variance-Based Radio Tomography Networks,” *arXiv. org*, 2009.

[4] M. Bocca, O. Kaltiokallio, N. Patwari, and S. Venkatasubramanian, “Multiple Target Tracking with RF Sensor Networks”, *arXiv.org*, 2013.

[5] D. Lieckfeldt, J. You, and D. Timmermann, “Characterizing the Influence of Human Presence on Bistatic Passive RFID-System,” *2009 IEEE Int. Conf. Wirel. Mob. Comput. Netw. Commun.*, 2009.

[6] B. Wagner and D. Timmermann, “Adaptive Clustering for Device Free User Positioning utilizing Passive RFID,” *4th Work. Context Syst. Des. Eval.*, 2013.

[7] K. S. Leong, M. L. Ng, A. R. Grasso, and P. H. Cole, “Dense RFID Reader Deployment in Europe using Synchronization,” *J. Commun.*, Dec. 2006.

[8] B. Wagner, B. Striebing, and D. Timmermann, “A System for Live Localization In Smart Environments,” *IEEE Int. Conf. Networking, Sens. Control*, 2013.

[9] T. Hastie, R. Tibshirani, and J. Friedman, *The Elements of Statistical Learning: Data Mining, Inference and Prediction, Second Edition*, Springer S. Springer, 2009.

[10] EPCGlobal Inc., “Specification for Air Interface EPC ™ Radio-Frequency Identity Protocols Class-1 Generation-2 UHF RFID Protocol for Communications at 860 MHz – 960 MHz,” 2008.

[11] “Kathrein RFID GmbH.” [Online]. Available: http://www.kathrein-rfid.de. [Accessed: 04-Jan-2014].

[12] “Alien Technology Inc.” [Online]. Available: http://www.alientechnology.com/. [Accessed: 04-Jan-2014].